



Since 1969



# Synthesis of $\text{MnO}_2$ Carbon Nanotubes Catalyst With Enhanced Oxygen Reduction Reaction for Polymer Electrolyte Membrane Fuel Cell

M. Sadiq<sup>1</sup>, M. Arif<sup>2\*</sup>, A. Ullah<sup>2</sup>, A. Naveed<sup>2</sup>, S. Afridi<sup>2</sup>, M. Humayun<sup>3</sup>, M. N. Khan<sup>4</sup>, M. Asif<sup>5</sup>

Submitted: 28/08/2021, Accepted: 05/10/2021, Online: 07/10/2021

## Abstract

Polymer Electrolyte Membrane Fuel Cell (PEMFC), an electrochemical power generating technology, uses a precious metal Platinum (Pt) catalyst for Oxygen Reduction Reaction (ORR), which is a major hindrance in its commercialization. Using a non-precious group metal (NPGM) instead of Pt will reduce the cost of PEMFCs. Herein  $\text{MnO}_2$  carbon nanotubes (CNTs) were synthesized by impregnating the transition metal in large surface carbonaceous material CNTs by hydrothermal synthesis techniques. To enhance the catalytic reaction and increase the volumetric current density, the sample was pyrolyzed at 800 °C temperature under nitrogen atmosphere. During pyrolysis, the nitrogen was also doped in the framework of carbonaceous materials. The materials were then treated with acid, removing the unreacted metals and adding oxygen functional group to the CNT framework due to which the activity of the catalyst is amplified. The catalysts have been characterized by scanning electron microscope (SEM), X-ray diffraction (XRD), Catalyst activity has been calculated by Rotating Disc Electrode (RDE) experiment. The resulting materials are stronger in experimental conditions in alkaline environment and have high electro catalytic activity for oxygen reduction reaction (ORR). Linear Sweep Voltammetry (LSV) depicts a current density of - 4.0 mA/cm<sup>2</sup> and over potential of -0.3V vs. Standard Calomel Electrode (SCE) in 0.1M KOH electrolyte. Rotating Disk Electrode (RDE) was conducted at 400, 800, 1200, and 1600 rpm. The results of  $\text{MnO}_2$  CNT show a desirable future aspect in fuel cell commercialization.

**Keywords:** Carbon nanotubes (CNTs), Polymer Electrolyte Membrane Fuel Cell (PEMFC), Oxygen reduction reaction.

## 1. Introduction:

The Polymer Electrolyte Membrane Fuel Cell (PEMFC) is a renewable energy technology that generates energy by Redox reaction of fuel (Hydrogen) and oxidant (oxygen) at opposite electrodes. It is better than internal combustion (IC) engines in term of its higher efficiency, zero carbon emission and neutral by product such as

water, that is why it may be viewed as a greener technology. Along with that, it has ease of refilling capabilities and larger operation time than batteries [1]. PEMFCs gained its popularity for powering vehicles and backup power system [2]. It is a state of the art technology with wide range of applications; however, this technology is facing various commercialization challenges in term of cost

<sup>1</sup>Department of Mechanical Engineering, University of Engineering and Technology Peshawar, Pakistan

<sup>2</sup>Center for Advanced studies in Energy, University of Engineering and Technology Peshawar, Pakistan

<sup>3</sup>Department of Basic sciences, University of Engineering and Technology, Peshawar, Pakistan

<sup>4</sup>Department of Electrical Engineering, Bannu Campus, University of Engineering and Technology, Peshawar, Pakistan

<sup>5</sup>Department of Electronics, University of Peshawar, Peshawar, Pakistan

**Corresponding Author:** arif.khattak@uetpeshawar.edu.pk

and durability [3, 4]. The use of Precious metal Platinum (Pt) as anode and cathode catalyst is the key reason for its expensiveness [4]. Currently, the high cost catalyst (Pt) is considered to be the half of the fuel cell cost [5]. The prices of Pt is conspicuously unstable and uncertain due to its uneven geographical distribution, as roughly 90% of the Pt is found in Russia and South Africa [6]. The unequal distribution creates a hustle and may cause a huge raise in its prices at any time.

Till date Pt inculcated in carbon black and Pt alloys are considered to be the efficient catalyst for PEMFCs [7, 8]. The oxygen reduction reaction (ORR) is sluggish at cathode side than the hydrogen oxidation reaction at anode, so it requires high activation sites and thus the loading at cathode is higher than the anode. The research is going on to develop more efficient, more active and more abundant cheap catalyst for ORR [9] and efforts are made by different researchers to replace the Pt catalyst with non-precious group metal (NPGM) catalyst. The NPGM catalyst should have high volumetric activity and durability in acidic medium [10]. The main problem of the NPGM is that it erodes away in acidic medium. The transition metals are strong candidates for replacing Pt as they have high stability in oxygen and peroxide environment and low over potential in 4e- oxygen to water reduction transfer, however, they have limited active sites. Despite the fact that the Pt metal is still a promising catalyst, but its high cost limits its use in commercial fuel cells. Research is imperative in finding the abundant transition metal having high volumetric activity and durability so that they can be used as alternative to Pt metal in Fuel cells [11]. Following the Jasinski's work on Cobalt (Co) as metal catalyst, research on metal and nitrogen embedded in the carbon (M/N/C) get started swiftly because their porous structure provide large surface area, high electrical conductivity and chemical stability with high thermal robustness [12]. Although carbon has intrinsically, less activity for Oxygen reduction reaction (ORR) but it is perceived that nitrogen engraving and non-precious metal impart catalytic actives due to production of actives site [13]. Fe

catalyst were also developed mimicking the idea of Fe hemocopper active center found in cytochrome oxidase in enzyme oxygen reduction in prokaryotes and mitochondria [14]. Nitrogen carbon nanotubes can be either directly doped in the synthesis process or can be doped after synthesis the as prepared sample consisting of metal atoms (Fe, Co, Mn, Ni) and nitrogen is imprinted on macro cyclic carbon compound which exhibits high ORR activity [15]. The macro cyclic carbon technic has been found offering good ORR activity, however, suffers stability, particularly in acidic environment. To enhance ORR activity, these material are also heat treated but very high temperature instigate acute losses i.e. reduces the active site densities, hence reduces the life time of catalyst [16]. But moderately high temperature causes expansion in the carbon structure forming Nanotubes, to which metals and nitrogen are engraved on the surface, the newly developed catalysts for fuel cells should have the following characteristics, volumetric activity is greater or equal to 1/10 that of Pt based catalyst, Excellent mass transport, High durability. Research has shown that the volumetric activity of M/N/C catalyst is lower than required value [18], but the loading of the NPGM can be increased to 1-5 mg/cm<sup>2</sup> as compared to Pt which is 0.1-0.4 mg/cm<sup>2</sup> and will be feasible technologically and economically, which will allow the required mass transport and activity.

In this study MnO<sub>2</sub> CNT nanocatalyst was synthesized using hydrothermal techniques. The crystal structure and morphology was studied using X-ray Diffraction and field emission scanning electron microscope respectively. Linear sweep voltammetry was conducted in 0.1M KOH electrolyte using Rotating disk electrode (RDE) to examine the ORR performance and durability of the catalyst in alkaline medium.

## **2. Characterization:**

X-Ray Diffractometer (model Phillip's analytical X-Ray PW 1830 Netherland Diffractometer with Cu K $\alpha$  radiation ( $\lambda$ =0.154nm, 40 kV and 30 mA) with step size of 0.05 degree and one second of dwell time was used to investigate the catalysts. The structure and morphology of catalysts were studied under

Field Emission Scanning Electron Microscope (Model HITACHI S-4700 FESEM). Linear sweep voltammetry (LSV) curves of catalyst were obtained by 3- Electrode Rotating Disk Electrode system (Model AFE3T0GC, Pine Instruments) having glassy carbon(GC) Electrode (4mm diameter).

### 3. Materials and Methods:

#### 3.1 Materials used:

Potassium permanganate ( $\text{KMnO}_4$ ), Carbon nanotubes (CNT), Deionized water (DI), Sulphuric acid, Nitric acid. All these chemicals were purchased from Sigma Aldrich (Shanghai, China). Deionized water ( $>18 \text{ M}\Omega \text{ cm}$ ) was used in all cleaning and rinsing procedures. All reagents mentioned above were used without further purification.

#### 3.2 Experimental Setup:

The  $\text{MnO}_2$  CNTs were prepared hydrothermally using Pristine Carbon nanotubes (CNTs) by impregnating  $\text{MnO}_2$  on CNTs through reduction pathway shown in the Fig 1. Before synthesizing, the CNTs were subjected to a 3:1 concentrated

Sulphuric acid to concentrated Nitric acid solution for 12 hours at ambient temperature for purification. The sample was then collected, washed with DI water simultaneously until the pH of the water became 7 and dried at  $120^\circ\text{C}$  for 12 h.

In the typical synthesis of  $\text{MnO}_2$  CNTs, 0.1g of the acid treated CNTs were dispersed in 25 ml DI water and put on ultrasonic sonicator for 2h. A 0.3g of Potassium permanganate ( $\text{KMnO}_4$ ) was added drop wise to the above sample and the solution were fully agitated by magnetic stirrer for 2h. The solution was then transferred to stainless steel autoclave; the autoclave was bolted and put in oven for 12 h and providing temperature of  $140^\circ\text{C}$ . A brown color sample was collected after cooling the autoclave naturally to ambient temperature by filtration, washed with DI water and dried at  $100^\circ\text{C}$  at vacuum environment. For preparation of  $\text{MnO}_2$  sample, 95% conc. 0.2 ml  $\text{H}_2\text{SO}_4$  was pipetted to 0.3g of  $\text{KMnO}_4$  solution in 25 ml DI water. The solution was then put in autoclave and sealed it tightly and put into electric oven at  $140^\circ\text{C}$  temperatures for 6h.

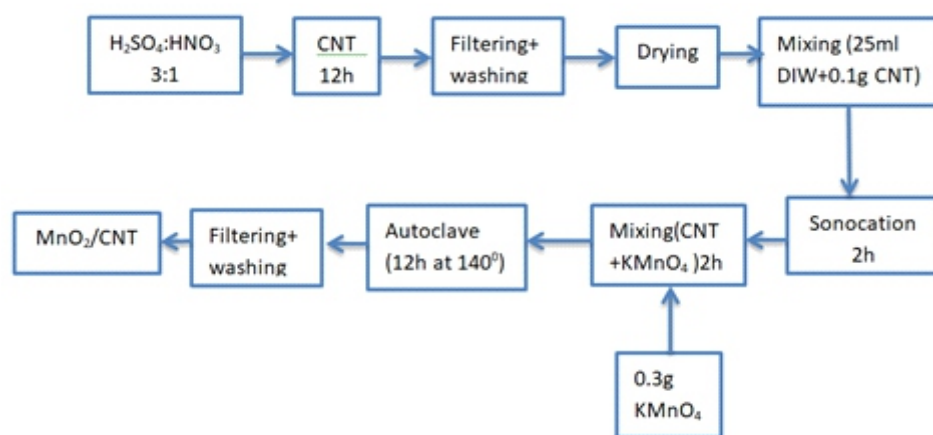


Figure 1: Hydrothermal synthesis of  $\text{MnO}_2$  CNT

#### 2.3 Electrode Preparation:

Catalytic electrode was prepared by dispersing 7.6 mg of  $\text{MnO}_2$  CNT sample in 7.6 ml of DI water.

Isopropanol of 2.4 ml and 40 $\mu\text{l}$  of Nafion was added to the solution and sonicated for 30 minutes.

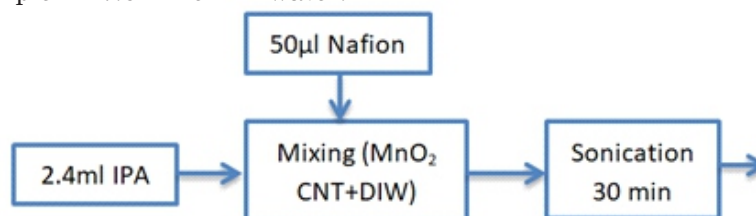
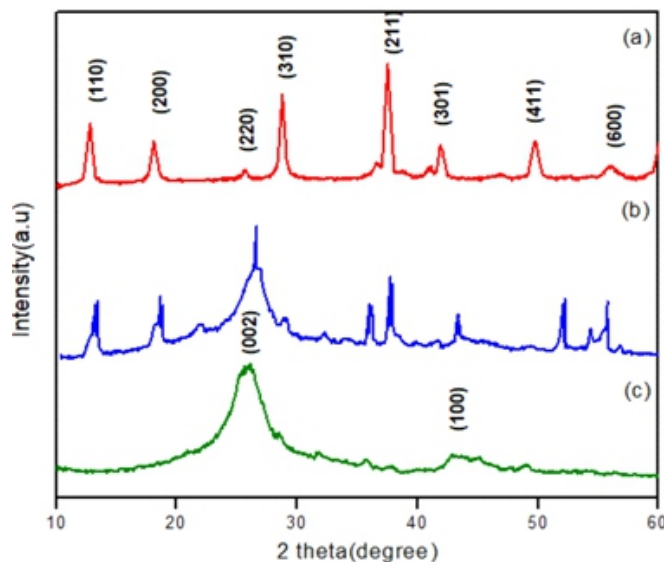


Figure 2: Preparation of  $\text{MnO}_2$  CNT Ink

#### 4. Results:

Figure.3 (a) shows the XRD patterns of  $\text{MnO}_2$  sample having no CNT which shows eight main peaks of (110), (200), (220), (310), (211), (301), (411), (600), showing that pure  $\text{MnO}_2$  crystals were formed based on comparison with JCPDS No 44-0141. Fig.3(c) shows the XRD patterns of CNT, high peaks were observed of (002), (100) at 2 theta values of  $26^\circ$

and  $42^\circ$  respectively of the CNT [24]. Figure.3 (b), (c) shows the XRD patterns of CNT,  $\text{MnO}_2\text{CNT}$  respectively. Except from the CNT characteristic peaks (002) and (100), all the other peaks could be indexed to the tetragonal phase of  $\text{MnO}_2$  (JCPDS No.44-0141) showing the  $\text{MnO}_2$  has been incorporated into  $\text{MnO}_2\text{CNT}$  hybrid sample.



**Figure.3:** XRD pattern of (a)  $\text{MnO}_2$ , (b) CNT, (c)  $\text{MnO}_2\text{CNT}$

The surface morphology of  $\text{MnO}_2$  and  $\text{MnO}_2\text{CNT}$  catalyst was studied using SEM as shown in Figure 4 (a) and (b) respectively. It was observed that  $\text{MnO}_2$  CNT catalyst has large size nanotubes ranging from 40 -100 nm, the oxide particle are smoothly dispersed on the nanotubes attached to the CNT backbone and having no agglomeration. The particle size has been reported [21] of significant role in enhancement of ORR. The  $\text{MnO}_2\text{CNT}$  outperform  $\text{MnO}_2$  electrochemically. The  $\text{MnO}_2$  catalyst nanorods have larger diameter ranging

from 0.01 to 0.1 micrometer with a clear agglomeration on the nanorods halting the catalytic activity shown in Figure 4 (a). The heat treatment transformed the Nano rods of short length and larger diameter to nanotubes of larger length and smaller diameter due to the effect of increasing temperature thus increased the aspect ratio of  $\text{MnO}_2\text{CNT}$ . The transformation increases the surface area, increasing the catalytic sites and ultimately enhancing the activity toward ORR in PEMFCs.

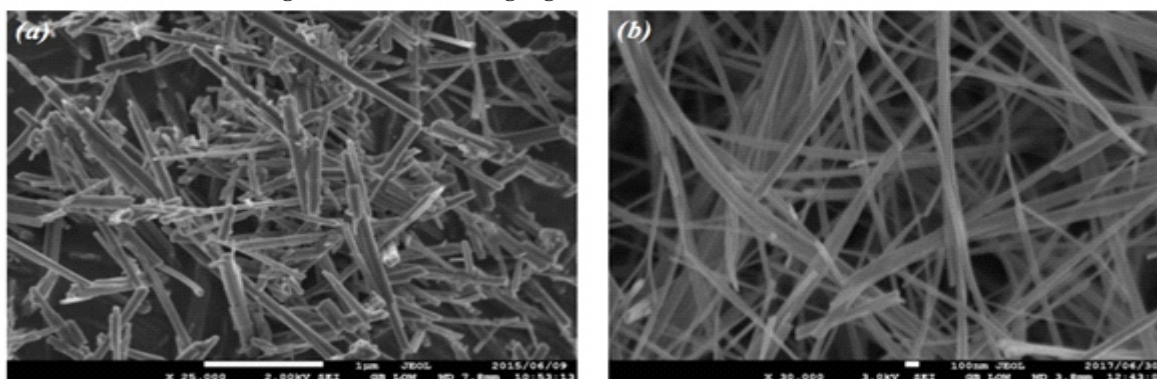


**Figure 4 (a):** SEM of  $\text{MnO}_2$  (b) SEM of  $\text{MnO}_2\text{CNT}$



### 3.1. ORR performance:

Figure.5 (a), (b), (c) shows the linear sweep voltammetry (LSV) curves of catalyst  $\text{MnO}_2$  CNT,  $\text{MnO}_2$  and commercial Pt/C in 0.1 M KOH electrolyte environment. The oxygen is purged for 30 minutes before the inception of the experiment [22, 23]. The  $\text{MnO}_2$  CNT curve depicts a substantial reduction current with a reduction peak at -0.2V (vs standard calomel electrode, SCE) in the oxygen saturated environment. The reduction peaks of  $\text{MnO}_2$  and commercial Pt/C occurred at -0.35V and -0.045V (vs SCE) respectively. The reduction potential of Pt/C is mere 0.08V positive than  $\text{MnO}_2$  CNT, which indicates that the catalytic activity of Pt/C is a modicum amount larger than  $\text{MnO}_2$  CNT. The reduction potential of  $\text{MnO}_2$  CNT shifts from -0.28 to -0.32 at 1600 rpm. The onset potential for the reduction current of  $\text{MnO}_2$  CNT is -0.2V and the order of onset potential for reduction current are Pt/C (-0.045V) >  $\text{MnO}_2$  CNT (-0.2V) >  $\text{MnO}_2$  (-0.35V).  $\text{MnO}_2$  CNT has more positive onset potential than  $\text{MnO}_2$  but insignificantly less than Pt/C catalyst. The onset potential is regarded as the indicator of the catalytic activity [24]. These results and comparison suggests that  $\text{MnO}_2$  CNT has higher catalytic activity, which might be associated with the nanotubes formation due to heat treatment, disordered morphology, higher edged structure resulting larger active sites, nitrogen doping in sintering and the addition of oxygen functional groups with CNT. The rotating disk electrode Voltammetry for  $\text{MnO}_2$  CNT at various rotation rate of 400, 800, 1200 and 1600 shown in Figure 5. (a) shows that an increase in current density can be seen with the rise in rotating speed and this is due to more oxygen diffusion and electron transfer number. The rotation rates were selected based on the optimized parametric data available in the literature.  $\text{MnO}_2$  current has the lowest current density ( $-2.5\text{mA}/\text{cm}^2$ ) at a reduction potential of -0.6V vs SCE shown in the Figure.5 (b), the commercial Pt/C has the highest current density of  $-4.6\text{mA}/\text{cm}^2$  in oxygen saturated environment with a Pt loading of  $45\mu\text{g}/\text{cm}^2$  at a reduction potential of -0.2 V (vs SCE) shown in the in Figure.5 (c).

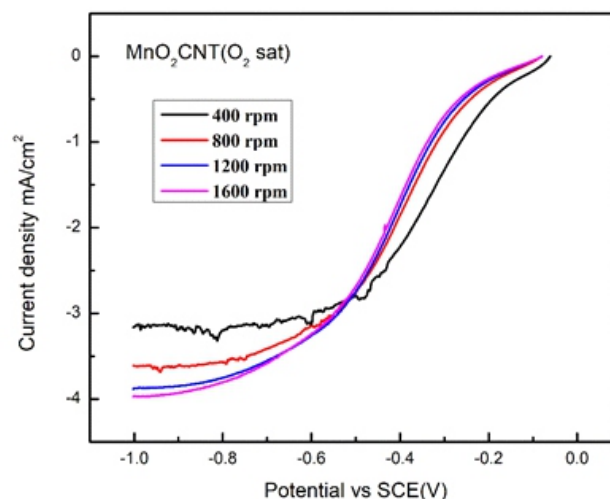


**Figure. 5 (a):** Polarization curve of heat treated  $\text{MnO}_2$  CNT ( $\text{O}_2$  sat. and 0.1M KOH)

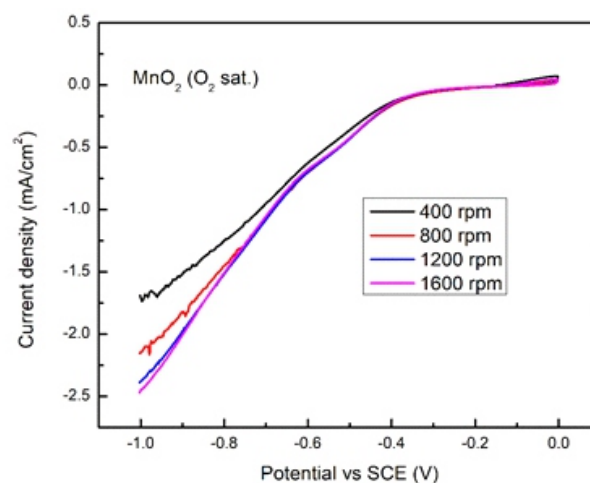


**Figure.5 (b):** Polarization curve of  $\text{MnO}_2$  ( $\text{O}_2$  sat. and 0.1M KOH)

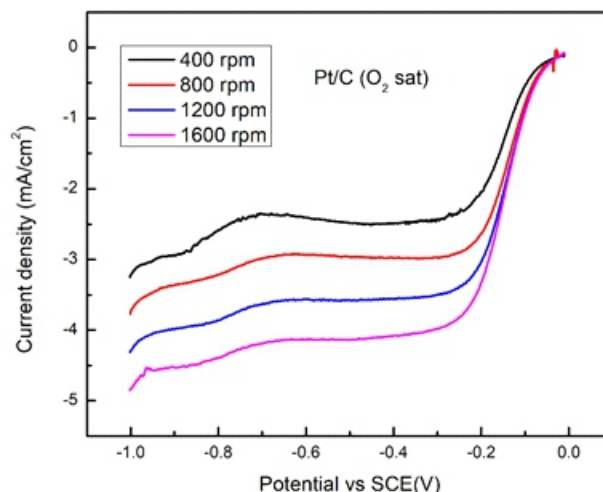


**Figure.5 (c):** Polarization curve of commercial Pt/C ( $\text{O}_2$  sat. and 0.1M KOH)

Figure 6 shows the LSV curve comparison between the catalytic activities of MnO<sub>2</sub> CNT, MnO<sub>2</sub> and commercial Pt/C catalysts at same environment and same revolution. Although Pt/C has high current density but it is clearly evident that the current density of the MnO<sub>2</sub> CNT

was enhanced with heat treatment due to structural expansion, the temperature was set at 140 °C. It is also conformed from XRD that there is a clear crystallographic growth at (002) and (100) indices, which is favorable for catalytic activity of ORR.

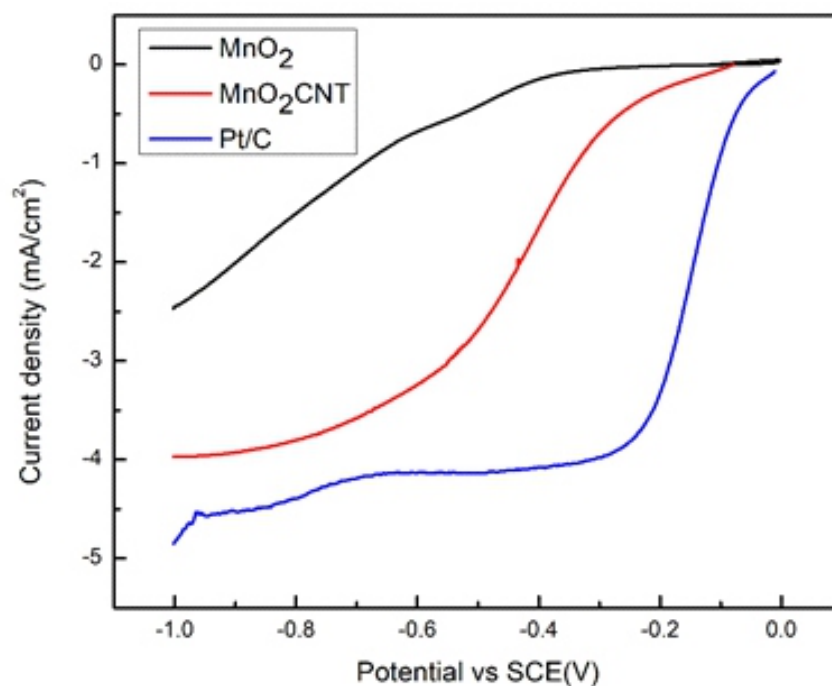
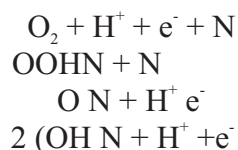
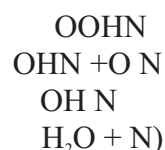


**Figure 6:** LSV comparison of MnO<sub>2</sub>, heat treated MnO<sub>2</sub>CNT, Pt/C (O<sub>2</sub> sat. and 0.1M KOH)

The reduction of oxygen to water proceeds in different ways, whether it proceeds in four electron transfer having water as end product or proceeds through two electron transfer forming peroxide



ions. For conformation the peroxide ion can be detected by testing the outflow water from the PEMFCs. The reaction of four-electron transfer proceeds in the following order



The number n of electron for oxygen reduction can be calculated using Koutecky-Levich (K-L) equation drawn from RDE data for various

voltages shown in fig 7. Equation (1), (2), (3) is used to calculate the electron transfer number. The K-L equation is as follow.

$$j^{-1} = j_L^{-1} L - 1 + j_k^{-1} \dots \dots \dots (1) \P$$

$$j^{-1} = (Bw^{1/2})^{-1} + j_k^{-1} \dots \dots \dots (2) \P$$

$$B = 0.62nFC_0(D_0)^{2/3} \nu^{-1/6} \dots \dots \dots (3) \P$$

Where  $J$  is the current density,  $j_K$  and  $j_L$  is the kinetic and diffusion limiting current density,  $w$  is the angular velocity of rotating disk,  $n$  is the electrons transferred in oxygen reduction. Here,  $F$  is the faraday constant ( $96485 \text{ Cmol}^{-1}$ ),  $C_0$  is the bulk concentration of oxygen ( $1.2 \times 10^{-6} \text{ mol cm}^{-3}$ ),  $\nu$

is the kinematic viscosity of electrolyte ( $0.01 \text{ cm}^2 \text{ s}^{-1}$ ) and  $D_0$  is the diffusion coefficient of  $\text{O}_2$  in  $0.1 \text{ M KOH}$  solution ( $1.9 \times 10^{-5} \text{ cm}^2 \text{ s}^{-1}$ ) [24]. First, the slope is calculated using the K-L plot shown in the figure 7, and then plugged the value in the equation to get electron transfer number.

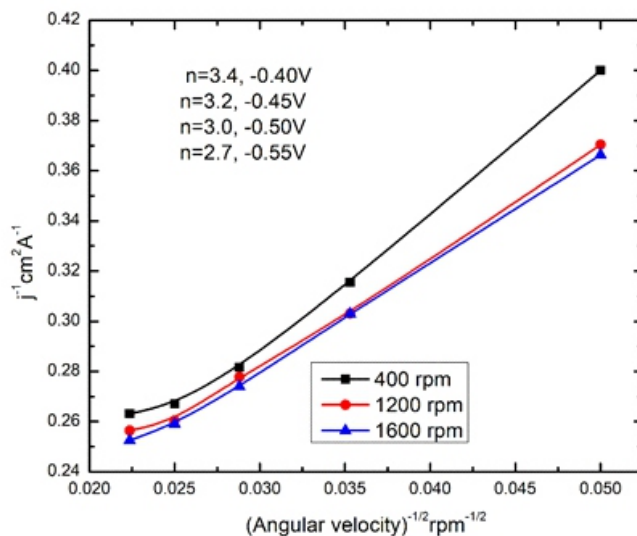


**Figure 7:** K-L plot for  $\text{MnO}_2/\text{CNT}$  at various potentials

Considering equation 1, 2 and 3 the electron transfer number was 3.4, 3.2, 3.0, 2.7 at potential of -0.4, -0.45, -0.50, -0.55 vs SCE. The result suggest that reaction will proceeds with four electron transfer at higher voltages producing water as end product, which depicts the catalyst is preferable in fuel cell at higher potential; on the other hand, at low potential the reaction prefer two electron transfer which is detrimental for fuel cell, it will

corrode away the catalyst in the high corrosive environment. However, it will be preferable for the other reaction in chemical industries i.e. production of peroxide ion. For corroboration the crystallite size, Full width half maximum (FWHM) technique is used to calculate the size of crystallite, it was calculated by the following method shown in the figure 8, the data acquired was then put in the equation 4 to calculate the diameter of crystallite.

$$D = K\lambda / (d \cos \theta) \dots \dots \dots (4)$$

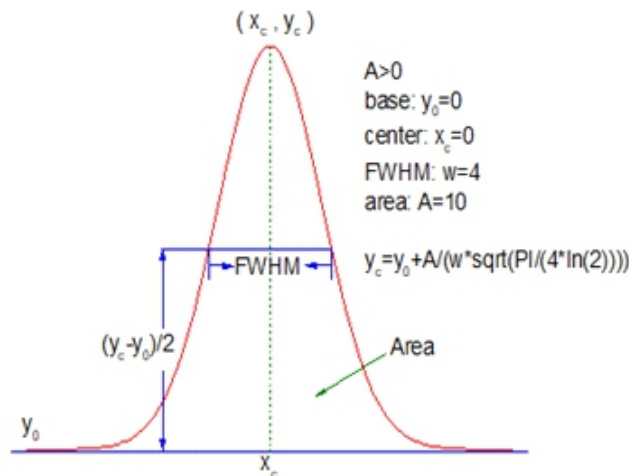


**Figure 8:** Graph for calculating of FWHM

D is the crystal size, K is shape factor close to unity (0.9),  $\lambda$  is the X-ray wave length ( $\lambda = 1.54060$  for Cu K $\alpha$ ),  $\Delta 2\theta$  is broadening at half maximum intensity (units are in radians),  $\theta$  is Bragg angle. From the above equation we have calculated crystals size ranging 6-7.5nm. They have broader peaks and smaller crystallite size, hence enhancing the surface area for catalyst site and catalytic activity ultimately. According to the average diffusion time equation (5)

$$T = \frac{r^2}{D} \pi^2 \dots \dots \dots (5)$$

Where D is the diameter, T is the time of diffusion and r is the radius of crystallite. Larger particle size of crystallite will lead to longer diffusion time and will delay reaction time; hence catalytic reactivity is proportional to the particle size. Herein crystallite size is small (40-100nm), exhibiting that MnO<sub>2</sub> CNT catalyst has higher reactivity which is obviously evidenced in Fig 5, which is promising candidate for ORR in PEMFCs.

#### 4. Conclusions:

MnO<sub>2</sub> CNT nanotubes were successfully synthesized by hydrothermal process. The heat treated MnO<sub>2</sub> CNT exhibits high catalytic activity of -4.0 mA/cm<sup>2</sup>, which is much higher than MnO<sub>2</sub> (-2.5 mA/cm<sup>2</sup>) and more or less comparable to commercial Pt/C catalyst (-4.6 mA/cm<sup>2</sup>). They have low onset potential with an avalanche of electron transfer at -0.3V. It has high surface area with a 40-100nm-crystallite structure size. The impregnating of Nitrogen and addition of oxygen functional group adds up the catalytic property to MnO<sub>2</sub> CNT. High intensity growth is located at (001) and (002) indices. It has high durability in alkaline medium. Electron transfer number is calculated to be 3.4, 3.2, 3.0, 2.7 e-, the reaction proceeds in both 2 and 4 electron pathways

#### References:

1. E.Proietti, F.Jaouen<sup>1</sup>, M.Lefèvre, N.Larouche<sup>1</sup>, J.Tian<sup>1</sup>, J.Herranz<sup>1</sup> & J.Dodelet. Iron-based cathode catalyst with enhanced power density in polymer electrolyte membrane fuel cells. *Nature* 1427 (2011).
2. US Department of Energy. Fuel Cell Technologies Market Report), 13–14, 2010.
3. R.F. Service, Hydrogen cars: fad or the future? *Science* 324, 1257–1259, 2009.
4. L. Schlapbach, Technology: hydrogen-fuelled vehicles. *Nature* 460, 809–811, 2009.
5. B.D. James, J.A. Kalinoski & K.N. Baum, Mass Production Cost Estimation for Direct H<sub>2</sub> PEM Fuel Cell Systems for Automotive Applications: ([http://www1.eere.energy.gov/hydrogenandfuelcells/pdfs/dti\\_80kW\\_fc\\_system\\_cost\\_analysis\\_report\\_2010.pdf](http://www1.eere.energy.gov/hydrogenandfuelcells/pdfs/dti_80kW_fc_system_cost_analysis_report_2010.pdf)) 2010.
6. J. Matthey, Market data charts (<http://www.platinum.matthey.com/publications/market-data-charts/platinum-charts>) 2011.
7. R.P. O'Hayre, S.- W. Cha, , W.G. Colella, & F.B. Prinz, Fuel cell fundamentals 2nd edn, John Wiley, 2009.
8. D. Tompsett, Proton Exchange Membrane Fuel Cells (eds David P. Wilkinson et al.) 1-60 (CRC, 2009).
9. K.K. Debe, A.K. Schmoeckel, G.D. Vernstrom & R. Atanasoski, High voltage stability of nanostructured thin film catalysts for PEM fuel cells. *J. Power Sources* 161, 1002–1011, 2006.
10. A. Morozan, B. Josselme & S. Palacin, Low-platinum and platinum-free catalysts for the oxygen reduction reaction at fuel cell cathodes. *Energy Environ. Sci.* 4, 1238–1254 2011.
11. Z.G. Zhao et al. In-situ formation of cobalt-phosphate oxygen-evolving complex anchored reduced graphene oxide nanosheets for oxygen reduction reaction. *Sci. Rep.* 3, 2263; doi: 10.1038/srep02263, 2013.
12. X.H. Liu et al. Hollow, spherical nitrogen-rich porous carbon shells obtained from a porous organic framework for the supercapacitor. *ACS Appl. Mater. Interf.* 5, 10280–10287, 2013.
13. K.P. Gong, F. Du, Z.H. Xia, M. Durstock &



- L.M. Dai Nitrogen-doped carbon nanotube arrays with high electrocatalytic activity for oxygen reduction. *Science* 323, 760–764, 2009.
14. S. Yoshikawa et al. Redox-coupled crystal structural changes in bovine heart cytochrome c oxidase. *Science* 280, 1723–1729, 1998.
15. G. Wu, K.L. More, C.M. Johnston & P. Zelenay, High-performance electrocatalysts for oxygen reduction derived from polyaniline, iron, and cobalt. *Science* 332, 443–447, 2011.
16. K. Parvez et al. Nitrogen-doped graphene and its iron-based composite as efficient electrocatalysts for oxygen reduction reaction. *ACS Nano* 6, 9541–9550, 2012.
17. P. Zhang et al., ZIF-derived in situ nitrogen-doped porous carbons as efficient metal-free electrocatalysts for oxygen reduction reaction. *Energy Environ. Sci.* 7, 442–450, 2014.
18. F. Jaouen et al., Recent advances in non-precious metal catalysis for oxygen reduction reaction in polymer electrolyte fuel cells. *Energy Environ. Sci.* 4, 114–130, 2011.
19. F. Jaouen, M. Lefèvre, J.P. Dodelet & M. Cai, Heat-treated Fe/N/C catalysts for O<sub>2</sub> electroreduction: are active sites hosted in micropores, *J. Phys. Chem. B* 110, 5553–5558, 2006.
20. A. Ignaszak, S. Ye, & E. Gyenge, A Study of the catalytic interface for O<sub>2</sub> electroreduction on Pt: the interaction between carbon support meso/microstructure and ionomer (Nafon) distribution. *J. Phys. Chem. C* 113, 298–307, 2008.
21. A. Moisala, G. Albert, Nasibulin, and E.I. Kauppinen. "The role of metal nanoparticles in the catalytic production of single-walled carbon nanotubes—a review." *Journal of Physics: condensed matter* 15, no. 42, 2003
22. S.S. Kocha, Z. Jason, K.C. Neyerlin, B.S. Pivovar, Influence of nafion on the electrochemical activity of Pt-based electrocatalysts. In: Meeting abstracts, no. 13, pp.1269e1269. The Electrochemical Society; 2012.
23. D.T. Sawyer, S. Andrzej, J.L. Roberts, *Electrochemistry for chemists*. 2nd ed. John Wiley and Sons; ISBN 978-0-471-59468-0, 1995.
24. W. Ding, L. Li, K. Xiong, Y. Wang, W. Li, Y. Nie, & Z. Wei, (2015). Shape fixing via salt recrystallization: a morphology-controlled approach to convert nanostructured polymer to carbon nanomaterial as a highly active catalyst for oxygen reduction reaction. *Journal of the American Chemical Society*, 137(16), 5414–5420.
25. Z. Yang, X.M. Zhou, H.G. Nie, Z. Yao, S.M. Huang, Facile Construction of Manganese Oxide Doped Carbon Nanotube Catalysts with High Activity for Oxygen Reduction, *Journal of Power Sources* 236 (2013) 238e249